

ER Mutations Affect the Localization of Plant-Specific Insert (PSI) B in *Arabidopsis* †

Tatiana Cardoso ¹, Susana Pereira ^{1,2}, José Pissarra ^{1,2} and Cláudia Pereira ^{1,2,*}

¹ Department of Biology, Faculdade de Ciências, Universidade do Porto, Rua do Campo Alegre, s/n, 4169-007 Porto, Portugal; up201505769@up.pt (T.C.); mspereir@fc.up.pt (S.P.); jpissarr@fc.up.pt (J.P.)

² GreenUPorto—Sustainable Agrifood Production Research Centre/Inov4Agro, Department of Biology, Faculty of Sciences, University of Porto, Rua do Campo Alegre, s/n, 4169-007 Porto, Portugal

* Correspondence: cpereira@fc.up.pt

† Presented at the 2nd International Electronic Conference on Plant Sciences—10th Anniversary of Journal Plants, 1–15 December 2021; Available online: <https://iecps2021.sciforum.net/>.

Abstract: The ER is considered the hub of the secretory pathway, as newly synthesized proteins are distributed to other organelles from this location. Accordingly, alterations of ER structure or organization may have an impact on protein trafficking or, at least, the way proteins exit the ER. In this work, we intended to explore this problem by combining *Arabidopsis thaliana* mutants with altered ER structure with the expression of known vacuolar markers. The mutants *nai GFP-h* and *leb-2 GFP-h*, both involved in ER body biogenesis, were selected from the NASC database and were transiently transformed with the vacuolar marker PSI B–mCherry. Our results showed that PSI B is more secreted in the *nai GFP-h* mutant, whereas, in the *leb-2 GFP-h* mutant, PSI B–mCherry is less secreted and mainly accumulated in the vacuole, showing an opposite behavior when comparing to PSI B expression in wildtype. Therefore, the *nai* mutation increased the secretion to the cell wall, whereas the *leb* mutation increased the accumulation in the vacuole. We discuss whether the alterations in the ER may play a role in these processes.

Keywords: plant-specific insert; protein trafficking; protein sorting; endoplasmic reticulum; *Arabidopsis thaliana*; electron microscopy; confocal microscopy



Citation: Cardoso, T.; Pereira, S.; Pissarra, J.; Pereira, C. ER Mutations Affect the Localization of Plant-Specific Insert (PSI) B in *Arabidopsis*. *Biol. Life Sci. Forum* **2022**, *11*, 8. <https://doi.org/10.3390/IECPS2021-11930>

Academic Editor: Fulai Liu

Published: 30 November 2021

Publisher's Note: MDPI stays neutral with regard to jurisdictional claims in published maps and institutional affiliations.



Copyright: © 2021 by the authors. Licensee MDPI, Basel, Switzerland. This article is an open access article distributed under the terms and conditions of the Creative Commons Attribution (CC BY) license (<https://creativecommons.org/licenses/by/4.0/>).

1. Introduction

The endomembrane trafficking system of eukaryotic cells is vital for important cellular functions, upholding cellular homeostasis and proliferation, as well as specific requirements characteristic of multicellular organisms [1,2]. The secretory pathway of plant cells has its gateway in the endoplasmic reticulum (ER). This adaptable and versatile organelle forms a three-dimensional network of continuous tubules and cisterns contacting several organelles in the cell, such as the plasma membrane (PM), the Golgi, endosomes, lysosomes, mitochondria, and peroxisomes. Accordingly, it coordinates with multiple membrane compartments along both the secretory and the endocytic pathways [3–5]. In plants, unlike what we see in yeast and animal cells, the ER is confined to a small space of the cytoplasm between the PM and the vacuolar membrane, while being extensively distributed and showing considerable movement in the cell [6,7]. Some organisms may even develop characteristic ER-derived structures, such as the ER bodies, which are spindle-like compartments for the accumulation of large amounts of β -glucosidase (PYK10), which may be involved in plant defense and are found in Brassicaceae plants and some related species [8,9]. Additionally, ER bodies may participate as intermediates of trafficking routes to the vacuole as a response to ER stress [10], highlighting the plasticity of this organelle in plants.

The conventional trafficking through the secretory pathway takes proteins from the ER and leads them through the Golgi apparatus until their final destination, which might be

the vacuole, other compartments, or the plasma membrane [11,12]. As plant cells have two different types of vacuoles (protein storage vacuoles (PSVs) and lytic vacuoles (LVs)) and both may coexist within the same cell [13,14], it is important to understand the mechanisms and regulation behind vacuolar trafficking, as vacuoles play a central role in plant cell homeostasis. Our laboratory has been using cardosin A and cardosin B as working models, which are well-characterized aspartic proteinases (APs) found in *Cynara cardunculus* [15,16]. Despite being highly similar regarding protein sequence, these enzymes accumulate in different cell compartments during plant development [16,17]. Cardosin A has been shown to accumulate in PSVs or LVs, depending on the development stage and specific cellular needs [17–20], whereas cardosin B is found extracellularly [16]. However, when expressed in *Arabidopsis thaliana* and *Nicotiana tabacum*, both cardosins A and B were detected in LVs [21–23]. Such characteristics make cardosins intriguing and provide solid evidence for their utility as reporters for the study of vacuolar trafficking and vacuolar sorting determinants (VSDs) in plants.

Plant-specific inserts (PSIs) consist of unique protein domains of about 100 amino acids [24,25]. A PSI is frequently described as “an enzyme within an enzyme”, since, when isolated and in vitro, it presents several functions such as acting as a detergent, mediating lipid membrane interactions, presenting putative antimicrobial activity, and inducing membrane permeabilization, along with membrane modulation [26–30]. Although its functions in cells still need to be clarified, some reports have associated the PSI domain with vacuolar targeting of the APs [21,26,30]. As novel unconventional routes for vacuolar sorting, where proteins are directly sorted to the LV from the ER [22,31–34], are being revealed, it is necessary to understand where the PSI fits in the complex network of vacuolar protein trafficking. Even though both the cardosin A PSI (PSI A) and the cardosin B PSI (PSI B) can direct the AP to the vacuole, the ways in which they do so differ greatly. The transport from the ER to the Golgi in PSI B-mediated sorting is COPII-dependent, whereas PSI A-mediated sorting is COPII-independent [35]. Moreover, despite PSIs being considered vacuolar sorting determinants given their abilities to mediate trafficking to the vacuole, little is known regarding the mechanisms controlling this sorting. To understand in more detail the mechanisms of PSI-mediated sorting, and since the ER seems to be a crucial checkpoint in these routes, we hypothesized if defects at the ER level lead to changes in protein sorting. Accordingly, using the Nottingham *Arabidopsis* Stock Center (NASC) database, we searched and selected *Arabidopsis thaliana* lines with mutations in genes leading to alterations in ER morphology and analyzed the expression and localization of the PSI domain. The *nai GFP-h* mutant presents a single base pair change mutation in the *NAI1* gene that regulates the development of ER bodies, resulting in the suppression of the formation of such structures [36]. The *leb-2 GFP-h* mutant has a mutation in a codon (CCT to TCT), which causes a P41S mutation in the PYK10/BGLU23 protein, leading to elongated ER bodies.

2. Material and Methods

2.1. Biological Material—Selection, Germination, and Growth Conditions

From the Nottingham *Arabidopsis* Stock Center (NASC), two *Arabidopsis thaliana* lines described as having defects in ER morphology or mutations in ER-resident proteins were selected: N69075 (*nai GFP-h*) [36] and N69081 (*leb-2 GFP-h*—unpublished). These lines also harbor a GFP-HDEL marker that allows ER visualization. Seeds from those lines, as well as a wildtype (WT; *col0*), were sown and germinated in plates containing MS (Mourashige and Skooge, Duchefa) medium with 1.5% (*w/v*) sucrose. Plants were kept for 48 h at 4 °C and, after stratification, were grown at 22 °C with 60% humidity and 16 h light over 8 h dark photoperiod (OSRAM L 36 W/77 e OSRAM L 36 W/840) at the intensity of 110 $\mu\text{mol}\cdot\text{m}^{-2}\cdot\text{s}$. After 12–15 days, seedlings were transferred to individual pots with fertilized substrate (SYRO PLANT) and grown under continuous light at 22 °C with 50–60% relative humidity and light intensity at 180 $\mu\text{mol}\cdot\text{m}^{-2}\cdot\text{s}$.

2.2. Vacuum Infiltration for Transient Transformation of *Arabidopsis thaliana* Seedlings

For transient transformation of *A. thaliana*, the protocol established by Bernat-Silvestre et al. [37] was adapted. Seeds from *A. thaliana* mutated lines and wildtype were sown and germinated in six-well plates and grown for 5 days under the conditions already described. For the transformation, *A. tumefaciens* harboring SP-PSI B-mCherry construct [35] was inoculated in LB medium with the appropriate antibiotics (kanamycin (50 µg/mL) and gentamicin (50 µg/mL)) and incubated for 24 h in agitation at 28 °C, until an OD₆₀₀ of 2.2. The culture was centrifuged for 15 min at 6000 × *g* at room temperature, and the pellet was resuspended in infiltration buffer (liquid MS medium with 0.005% (*v/v*) Tween and 200 µM acetosyringone). This suspension was kept at room temperature for 30–45 min, and then poured onto the six-well plates with the *A. thaliana* seedlings (4 mL per well); next, a vacuum was applied at 300 mbar for 1 min. The pressure was then slowly increased to 400 mbar, and a vacuum was applied for another minute. Finally, the bacterial suspension was removed, and the plates were covered with aluminum foil for 45 min to 1 h to improve agro-infection. The aluminum foil was then removed, and the plates were kept for 3 days under the previously mentioned growth conditions.

2.3. Drug Treatment Assays

Brefeldin A (BFA) solution (50 µg/mL) was prepared in MS liquid medium, and 4 mL per well was poured over the infiltrated seedlings 1 day after the *A. tumefaciens* infiltration. A vacuum was applied as previously described (Section 2.2). Seedlings were kept in the BFA solution for about 16–18 h before the cells were imaged.

2.4. CLSM Analysis

A. thaliana seedlings were observed and analyzed using a confocal laser scanning microscope (CLSM, Leica STELLARIS 8). Cotyledons from *A. thaliana* seedlings were prepared by placing the biological material on a slide with a drop of sterile water covered by a cover slip. In all situations, the abaxial epidermis was observed. For mCherry, using 561 nm excitation, emissions were detected between 580 and 630 nm. In the case of GFP, the excitation wavelength used was 488 nm, and the emissions were detected between 500 and 528 nm. Analysis and quantification of the acquired images were performed using the ImageJ[®]/Fiji software.

2.5. Extraction of Extracellular Proteins

Agro-infiltrated and BFA-infiltrated seedlings were cut into thin strips and incubated in 1 × extraction buffer (0.1 M NaCl, 4 mM HEPES pH 7.0, 0.5 mM DTT, and 0.2 mM EDTA) under agitation (120 rpm) for 6 h at room temperature in the dark. A volume of 1 mL of buffer was used per 100 mg of seeding tissue. After incubation, the buffer was collected, filtered with a 100 µm nylon mesh, and centrifuged at 13,000 × *g* for 10–15 min at 4 °C. The supernatant was collected and kept at –20 °C. To the defrosted extracellular samples, 1 mL of 20% (*w/v*) trichloroacetic acid (TCA) was added per mL of medium, and the tubes were vortexed for 15 s. These were kept on ice for 15 min before centrifugation at 13,000 × *g* for 15 min at 4 °C. The supernatant was discarded, 1 mL of ice-cold acetone was added to the pellet, and the tubes were centrifuged as before. This wash was repeated, and the pellet was left to air-dry. The pellet was resuspended in 40 µL of extraction buffer, and the samples were quantified in a DS-11 Spectrophotometer (DeNovix). SDS-PAGE sample loading dye (Nzytech) was added, and samples were boiled at 95 °C for 5 min before being centrifuged for 2 min at top speed.

2.6. Western Blot Analysis

A 12% SDS-PAGE coupled to Western blotting was performed for the analysis of extracellular proteins samples, as described previously [35]. The same protein amount of each sample was applied to the gel along with the protein weight marker PageRuler Plus Prestained Protein Ladder (Thermo Fisher, Waltham, MA, USA). For the blot, the

primary antibodies—anti-mCherry (Merk Millipore, Burlington, MA, USA) and H3 Histone 3 core (Agrisera, Vännäs, Sweden)—were diluted (1:1000 and 1:5000, respectively) in blocking solution (5% (*w/v*) skim milk and 0.5% (*v/v*) Tween-20 in TBS-T), and incubation was performed at 4 °C overnight with agitation. The incubation with the secondary antibodies—goat anti-rabbit IgG (H + L) HRP conjugate and goat anti-mouse IgG (H + L) HRP conjugate (BioRad, Hercules, CA, USA), diluted in TBS-T (1:2500 and 1:500, respectively)—occurred at room temperature for 1 h in agitation. The visualization of the bands was carried out using the Clarity ECL Western Blotting Substrate Kit (BioRad), following the manufacturer's instruction; the imaging was acquired with a ChemiDoc XRS+ System (BioRad), and the analysis was performed using the ImageJ[®] software.

3. Results

The heterologous expression of the PSI B in *Arabidopsis* allowed us to assess the localization of this domain in the cell. Several images of each condition were captured and analyzed, and the most representative are presented. Moreover, a quantitative approach of the PSI B localization is also shown, giving a more complete perception of the patterns observed.

3.1. Expression and Localization of PSI B in ER-Defective Plants

Some differences were observed between WT and mutant lines regarding PSI B localization. In the WT line, PSI B was mostly observed accumulating in the vacuole, and, in some cells, it was also secreted to the cell wall (Figure 1A; arrows). In *nai GFP-h*, PSI B was found to be mostly secreted to the cell wall (Figure 1B; arrows), although some accumulation in the vacuole was still observed. In *leb-2 GFP-h*, PSI B was mainly accumulated in the vacuole (Figure 1C). Quantification of the distribution patterns observed for these lines showed a clear tendency for more secretion in the *nai GFP-h* line, when compared to the control, while, in the *leb-2 GFP-h*, less secretion was observed (Figure 2A).

Next, we assessed if Brefeldin A (BFA) affected these accumulation patterns. BFA is a fungal macrocyclic lactone widely used as an inhibitor of secretion and vacuolar protein transport in plant cells, causing the formation of ER–Golgi hybrid compartments [38]. Upon addition of the drug, the secretion observed in the untreated condition was decreased, but some accumulation in the cell wall was still visible (Supplementary Figure S1). The *nai GFP-h* line presented the PSI B in the vacuole and secreted. However, in the *leb-2 GFP-h*, the PSI B was only found to accumulate in the vacuole (Supplementary Figure S1). In the WT, this secretion was decreased after BFA treatment as in the *nai GFP-h* lines, and, in the *leb-2 GFP-h*, there was no secretion at all to the cell wall, as can be appreciated in the quantification (Figure 2B).

3.2. Secretion Assays

Given the extended secretion observed in some lines expressing PSI B, we decided to further confirm this event by isolating the extracellular protein content of seedlings from the WT and mutated lines infiltrated with PSI B fused with mCherry, with and without BFA. In this assay, a double control system was used; the control sample was an extract of the total protein content of seedlings that stably express the PSI B (unpublished data) and, to ensure that the bands obtained were not from intracellular proteins, an antibody against the H3 histone, a protein exclusively found in the intracellular content, was also used in the same protein extracts. Indeed, as observed through confocal microscopy, the PSI B–mCherry, with an expected size of 37 kDa, was detected in the extracellular protein content of the *nai GFP-h* and *leb-2 GFP-h* lines infiltrated with this domain (Figure 3).

Moreover, the decrease in secretion observed in CLSM imaging upon BFA treatment was also confirmed by the Western blot (Figure 3, lines “–” and “+” BFA). However, regarding the WT line, PSI B was only faintly detected in the blot for both situations analyzed (with and without BFA treatment). The histone H3 had an expected size of 17 kDa and was not detected in the samples of extracellular proteins.

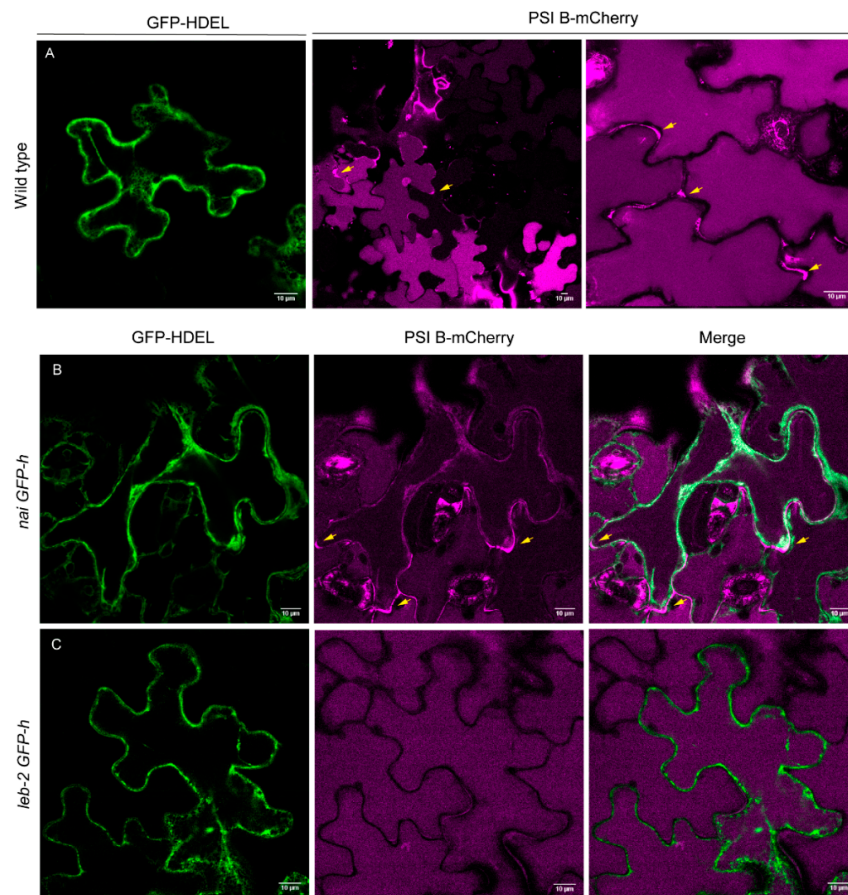


Figure 1. Subcellular localization of PSI B–mCherry in cotyledons of *Arabidopsis thaliana* wildtype and ER-defective seedlings. (A) Wildtype seedlings; pattern of GFP-marked ER and expression of PSI B–mCherry, which accumulated mostly in the vacuole, although some secretion to the cell wall was also observed. (B) In *nai GFP-h* seedlings, PSI B–mCherry was mainly secreted (arrows), although a limited accumulation could be detected in the vacuole. (C) In *leb-2 GFP-h* seedlings, PSI B–mCherry accumulated mainly in the vacuole. All observations and images were acquired 3 days post infiltration. Scale bars: 10 μ m.

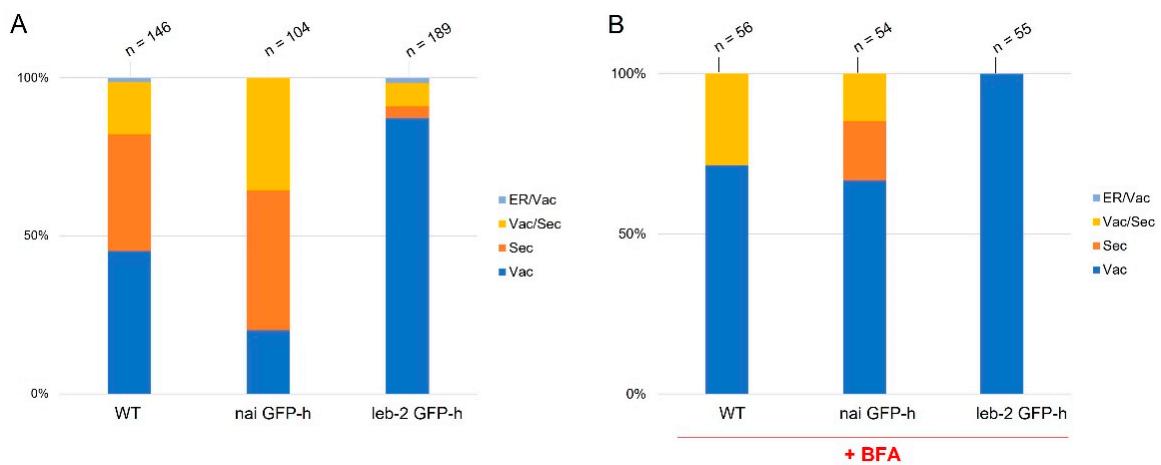


Figure 2. Quantification of PSI B in cotyledons of *Arabidopsis thaliana* wildtype and ER-defective seedlings in control conditions (A) and upon BFA treatment (B). The *n* above the bars refers to the number of cells counted. The PSIs were considered “secreted” when found at the cell periphery (cell wall). Abbreviations: ER, endoplasmic reticulum; Sec, secreted; Vac, vacuole.

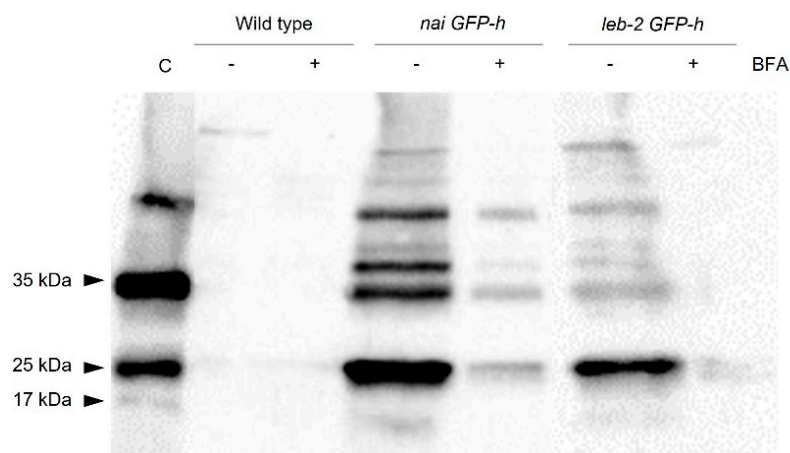


Figure 3. Detection of PSI B-mCherry in extracellular protein extracts from *Arabidopsis thaliana* wildtype and mutated lines. Western blot using a specific antibody against mCherry and Histone H3 (as a burst control). The arrows indicate the bands corresponding to the PSI B-mCherry (35 kDa), the isolated mCherry (25 kDa), and the histone H3 (17 kDa). The minus sign indicates the absence of BFA treatment, and the plus sign indicates the presence of BFA treatment. Abbreviations: C, control sample.

4. Discussion

For the past years, cardosins and their PSI domains have been the focus of several studies, given their contributions to unveil unconventional vacuolar sorting routes [22,35]. In fact, the PSI B domain can direct proteins to the vacuole but does not match any classical VSD type. Moreover, the route mediated by the PSI B is COPII-dependent and follows the conventional ER-Golgi-vacuole pathway [35]. In *Cynara cardunculus*, cardosin B is accumulated in the extracellular matrix of both stigma and style transmitting tissue [16], while, in heterologous systems (*Arabidopsis* and tobacco), it is accumulated in the LVs [23]. Such features highlight the advantage of this domain as a reporter for the study of vacuolar trafficking and VSDs in plants.

We started this study by assessing if the ER defects exhibited by the mutated lines had any influence on the localization and trafficking of PSI B. Results obtained revealed that, in the WT line, the major site for this domain's accumulation was the vacuolar compartment. However, some PSI B was also secreted to the cell wall. Interestingly, the two mutated lines observed show variations of this phenotype; in the *leb-2 GFP-h*, mutant PSI B mainly accumulated in the vacuole, while, in *nai GFP-h*, it was found to be mostly secreted. Although more information is needed to fully understand how alterations in the ultrastructure influence how the proteins leave ER, the shift toward the vacuole or cell wall indicates that the ER integrity is indeed crucial for signal recognition. The work of Soares da Costa and coworkers [23] described cardosin B's accumulation in the LVs, but the authors also mentioned its detection at the cell wall. Given its location in the native system (*Cynara cardunculus*), cardosin B's secretion has been suggested to be tissue-specific [18], with cardosin B being secreted in specialized organs, such as flowers and seeds, as well as in vacuoles in vegetative tissues, as in the case of fully expanded leaves (Figure 4, routes 1 and 2, respectively). It is worth noting that the images presented here correspond to cotyledonary cells, and we may argue that these cells constitute a transition stage with characteristics and cellular machinery of both embryonic tissue and vegetative tissue. Nevertheless, it seems an interesting stage to uncover the mechanisms of PSI B in more detail and, as a consequence, cardosin B-mediated sorting. In fact, the involvement of ER bodies in PSI B-mediated trafficking remains to be fully elucidated, particularly in seeds (Figure 4), where PSI B accumulates in PSVs of embryo cells. As a whole, this work provides new insights into this pathway and how it is influenced by the structure and physiology of the organelles, such as defects in ER morphology or mutations in ER-resident proteins.

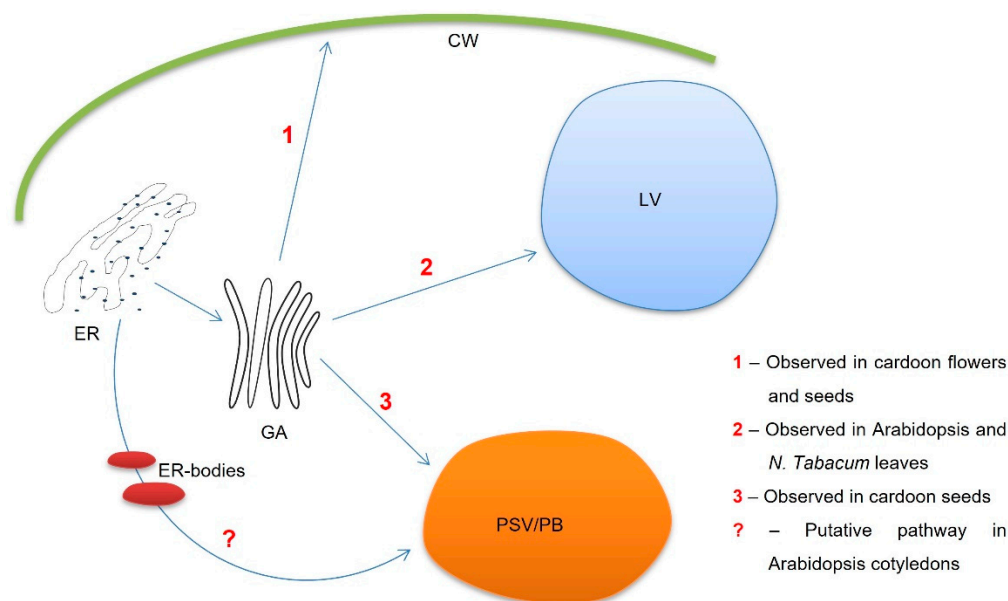


Figure 4. Schematic representation of the different PSI B-mediated protein trafficking routes in both native (*Cynara cardunculus*) and heterologous systems (*Arabidopsis thaliana* and *Nicotiana tabacum*).

Supplementary Materials: The following supporting information can be downloaded at: <https://www.mdpi.com/article/10.3390/IECPS2021-11930/s1>, Figure S1: Subcellular localization of PSI B-mCherry in cotyledons of *Arabidopsis thaliana* wild type and ER-defective seedlings treated with BFA.

Author Contributions: Conceptualization and methodology, S.P. and C.P.; investigation, T.C.; formal analysis and software, T.C. and C.P.; project administration and funding acquisition, J.P.; writing—original draft, T.C. and C.P.; writing—review and editing, S.P. and J.P.; supervision, S.P., J.P. and C.P. All authors read and agreed to the published version of the manuscript.

Funding: This research was performed in the frame of the scientific project PTDC/BIAFBT/32013/2017, funded by the Portuguese Foundation for Science and Technology (FCT) and supported by national funds through FCT, within the scope of UIDB/05748/2020 and UIDP/05748/2020.

Institutional Review Board Statement: Not applicable.

Informed Consent Statement: Not applicable.

Conflicts of Interest: The authors declare no conflict of interest.

References

- Morita, M.T.; Shimada, T. The Plant Endomembrane System—A Complex Network Supporting Plant Development and Physiology. *Plant Cell Physiol.* **2014**, *55*, 667–671. [\[CrossRef\]](#) [\[PubMed\]](#)
- Cevher-Keskin, B. Endomembrane Trafficking in Plants. *Electrodialysis* **2020**, 1–22. [\[CrossRef\]](#)
- Staehelin, L.A. The plant ER: A dynamic organelle composed of a large number of discrete functional domains. *Plant J.* **1997**, *11*, 1151–1165. [\[CrossRef\]](#) [\[PubMed\]](#)
- Stefan, C.J.; Manford, A.G.; Emr, S.D. ER-PM connections: Sites of information transfer and inter-organelle communication. *Curr. Opin. Cell Biol.* **2013**, *25*, 434–442. [\[CrossRef\]](#) [\[PubMed\]](#)
- Stefano, G.; Renna, L.; Lai, Y.; Slabaugh, E.; Mannino, N.; Buono, R.A.; Otegui, M.S.; Brandizzi, F. ER network homeostasis is critical for plant endosome streaming and endocytosis. *Cell Discov.* **2015**, *1*, 15033. [\[CrossRef\]](#)
- Nakano, R.T.; Matsushima, R.; Ueda, H.; Tamura, K.; Shimada, T.; Li, L.; Hayashi, Y.; Kondo, M.; Nishimura, M.; Hara-Nishimura, I. GNOM-LIKE1/ERMO1 and SEC24a/ERMO2 Are Required for Maintenance of Endoplasmic Reticulum Morphology in *Arabidopsis thaliana*. *Plant Cell* **2009**, *21*, 3672–3685. [\[CrossRef\]](#)
- Quader, H.; Schnepf, E. Endoplasmic reticulum and cytoplasmic streaming: Fluorescence microscopical observations in adaxial epidermis cells of onion bulb scales. *Protoplasma* **1986**, *131*, 250–252. [\[CrossRef\]](#)
- Matsushima, R.; Hayashi, Y.; Yamada, K.; Shimada, T.; Nishimura, M.; Hara-Nishimura, I. The ER Body, a Novel Endoplasmic Reticulum-Derived Structure in *Arabidopsis*. *Plant Cell Physiol.* **2003**, *44*, 661–666. [\[CrossRef\]](#)

9. Hara-Nishimura, I.; Matsushima, R.; Shimada, T.; Nishimura, M. Diversity and Formation of Endoplasmic Reticulum-Derived Compartments in Plants. Are These Compartments Specific to Plant Cells? *Plant Physiol.* **2004**, *136*, 3435–3439. [[CrossRef](#)]
10. Sampaio, M.; Neves, J.; Cardoso, T.; Pissarra, J.; Pereira, S.; Pereira, C. Coping with Abiotic Stress in Plants—An Endomembrane Trafficking Perspective. *Plants* **2022**, *11*, 338. [[CrossRef](#)]
11. Marcos Lousa, C.; Gershlick, D.C.; Denecke, J. Mechanisms and Concepts Paving the Way towards a Complete Transport Cycle of Plant Vacuolar Sorting Receptors. *Plant Cell* **2012**, *24*, 1714–1732. [[CrossRef](#)] [[PubMed](#)]
12. Rojo, E.; Denecke, J. What is moving in the secretory pathway of plants? *Plant Physiol.* **2008**, *147*, 1493–1503. [[CrossRef](#)] [[PubMed](#)]
13. Olbrich, A.; Hillmer, S.; Hinz, G.; Oliviusson, P.; Robinson, D.G. Newly formed vacuoles in root meristems of barley and pea seedlings have characteristics of both protein storage and lytic vacuoles. *Plant Physiol.* **2007**, *145*, 1383–1394. [[CrossRef](#)] [[PubMed](#)]
14. Paris, N.; Stanley, C.M.; Jones, R.L.; Rogers, J.C. Plant Cells Contain Two Functionally Distinct Vacuolar Compartments. *Cell* **1996**, *85*, 563–572. [[CrossRef](#)]
15. Ramalho-Santos, M.; Verissimo, P.; Cortes, L.; Samyn, B.; Van Beeumen, J.; Pires, E.; Faro, C. Identification and proteolytic processing of procarnosin A. *Eur. J. Biochem.* **1998**, *255*, 133–138. [[CrossRef](#)] [[PubMed](#)]
16. Vieira, M.; Pissarra, J.; Verissimo, P.; Castanheira, P.; Costa, Y.; Pires, E.; Faro, C. Molecular cloning and characterization of cDNA encoding cardosin B, an aspartic proteinase accumulating extracellularly in the transmitting tissue of *Cynara cardunculus* L. *Plant Mol. Biol.* **2001**, *45*, 529–539. [[CrossRef](#)]
17. Ramalho-Santos, M.; Pissarra, J.; Verissimo, P.; Pereira, S.; Salema, R.; Pires, E.; Faro, C.J. Cardosin A, an abundant aspartic proteinase, accumulates in protein storage vacuoles in the stigmatic papillae of *Cynara cardunculus* L. *Planta* **1997**, *203*, 204–212. [[CrossRef](#)]
18. Pissarra, J.; Pereira, C.; Soares, D.; Figueiredo, R.; Duarte, P.; Teixeira, J.; Pereira, S.; da Costa, D.S.; Figueiredo, R.; Duarte, P.; et al. From Flower to Seed Germination in *Cynara cardunculus*: A Role for Aspartic Proteinases. *Int. J. Plant Dev. Biol.* **2007**, *1*, 274–281.
19. Pereira, C.S.; da Costa, D.S.; Pereira, S.; de Moura Nogueira, F.; Albuquerque, P.M.; Teixeira, J.; Faro, C.; Pissarra, J. Cardosins in postembryonic development of cardoon: Towards an elucidation of the biological function of plant aspartic proteinases. *Protoplasma* **2008**, *232*, 203–213. [[CrossRef](#)]
20. Oliveira, A.; Pereira, C.; da Costa, D.S.; Teixeira, J.; Fidalgo, F.; Pereira, S.; Pissarra, J. Characterization of aspartic proteinases in *C. cardunculus* L. callus tissue for its prospective transformation. *Plant Sci.* **2010**, *178*, 140–146. [[CrossRef](#)]
21. Duarte, P.; Pissarra, J.; Moore, I. Processing and trafficking of a single isoform of the aspartic proteinase cardosin A on the vacuolar pathway. *Planta* **2008**, *227*, 1255–1268. [[CrossRef](#)] [[PubMed](#)]
22. Pereira, C.; Pereira, S.; Satiat-Jeunemaitre, B.; Pissarra, J. Cardosin A contains two vacuolar sorting signals using different vacuolar routes in tobacco epidermal cells. *Plant J.* **2013**, *76*, 87–100. [[CrossRef](#)] [[PubMed](#)]
23. da Costa, D.S.; Pereira, S.; Moore, I.; Pissarra, J. Dissecting cardosin B trafficking pathways in heterologous systems. *Planta* **2010**, *232*, 1517–1530. [[CrossRef](#)] [[PubMed](#)]
24. Simões, I.; Faro, C. Structure and function of plant aspartic proteinases. *Eur. J. Biochem.* **2004**, *271*, 2067–2075. [[CrossRef](#)] [[PubMed](#)]
25. Soares, A.; Ribeiro Carlton, S.M.; Simões, I. Atypical and nucellin-like aspartic proteases: Emerging players in plant developmental processes and stress responses. *J. Exp. Bot.* **2019**, *70*, 2059–2076. [[CrossRef](#)]
26. Egas, C.; Lavoura, N.; Resende, R.; Brito, R.M.M.; Pires, E.; de Lima, M.C.P.; Faro, C. The Saposin-like Domain of the Plant Aspartic Proteinase Precursor Is a Potent Inducer of Vesicle Leakage. *J. Biol. Chem.* **2002**, *275*, 38190–38196. [[CrossRef](#)]
27. Terauchi, K.; Asakura, T.; Ueda, H.; Tamura, T.; Tamura, K.; Matsumoto, I.; Misaka, T.; Hara-Nishimura, I.; Abe, K. Plant-specific insertions in the soybean aspartic proteinases, soyAP1 and soyAP2, perform different functions of vacuolar targeting. *J. Plant Physiol.* **2006**, *163*, 856–862. [[CrossRef](#)]
28. De Moura, D.C.; Bryksa, B.C.; Yada, R.Y. In silico insights into protein-protein interactions and folding dynamics of the saposin-like domain of *Solanum tuberosum* aspartic protease. *PLoS ONE* **2014**, *9*, 18–22. [[CrossRef](#)]
29. Frey, M.E.; D’Ippolito, S.; Pepe, A.; Daleo, G.R.; Guevara, M.G. Transgenic expression of plant-specific insert of potato aspartic proteases (StAP-PSI) confers enhanced resistance to *Botrytis cinerea* in *Arabidopsis thaliana*. *Phytochemistry* **2018**, *149*, 1–11. [[CrossRef](#)]
30. Muñoz, F.; Palomares-Jerez, M.F.; Daleo, G.; Villalain, J.; Guevara, M.G. Possible mechanism of structural transformations induced by StAsp-PSI in lipid membranes. *Biochim. Biophys. Acta—Biomembr.* **2014**, *1838*, 339–347. [[CrossRef](#)]
31. De Caroli, M.; Lenucci, M.S.; Di Sansebastiano, G.-P.; Dalessandro, G.; De Lorenzo, G.; Piro, G. Protein trafficking to the cell wall occurs through mechanisms distinguishable from default sorting in tobacco. *Plant J.* **2011**, *65*, 295–308. [[CrossRef](#)] [[PubMed](#)]
32. De Marchis, F.; Bellucci, M.; Pompa, A. Unconventional pathways of secretory plant proteins from the endoplasmic reticulum to the vacuole bypassing the Golgi complex. *Plant Signal. Behav.* **2013**, *8*, e25129. [[CrossRef](#)] [[PubMed](#)]
33. Stigliano, E.; Faraco, M.; Neuhaus, J.-M.M.; Montefusco, A.; Dalessandro, G.; Piro, G.; Di Sansebastiano, G.-P. Pietro Two glycosylated vacuolar GFPs are new markers for ER-to-vacuole sorting. *Plant Physiol. Biochem.* **2013**, *73*, 337–343. [[CrossRef](#)] [[PubMed](#)]
34. Di Sansebastiano, G.P.; Barozzi, F.; Piro, G.; Denecke, J.; Lousa, C.D.M. Trafficking routes to the plant vacuole: Connecting alternative and classical pathways. *J. Exp. Bot.* **2018**, *69*, 79–90. [[CrossRef](#)] [[PubMed](#)]
35. Vieira, V.; Peixoto, B.; Costa, M.; Pereira, S.; Pissarra, J.; Pereira, C. N-linked glycosylation modulates Golgi-independent vacuolar sorting mediated by the plant specific insert. *Plants* **2019**, *8*, 312. [[CrossRef](#)]

36. Matsushima, R.; Fukao, Y.; Nishimura, M.; Hara-Nishimura, I. NAI1 gene encodes a basic-helix-loop-helix-type putative transcription factor that regulates the formation of an endoplasmic reticulum-derived structure, the ER body. *Plant Cell* **2004**, *16*, 1536–1549. [[CrossRef](#)]
37. Bernat-Silvestre, C.; De Sousa Vieira, V.; Sánchez-Simarro, J.; Aniento, F.; Marcote, M.J. Transient Transformation of *A. thaliana* Seedlings by Vacuum Infiltration. *Methods Mol. Biol.* **2021**, *2200*, 147–155. [[CrossRef](#)]
38. Nebenführ, A.; Ritzenthaler, C.; Robinson, D.G. Brefeldin A: Deciphering an enigmatic inhibitor of secretion. *Plant Physiol.* **2002**, *130*, 1102–1108. [[CrossRef](#)]